INFLUENCE OF GRID TOPOLOGY ON THE OPERATING ENVELOPE USING RELAXED THREE-PHASE OPF

Lionel Delchambre[1*], Patrick Hendrick[2], Pierre Henneaux[1]

[1] *BEAMS dept. Université libre de Bruxelles (ULB), Brussels, Belgium*
[2] *ATM dept. Université libre de Bruxelles (ULB), Brussels, Belgium*
**lionel.delchambre@ulb.be*

Keywords: OPERATING ENVELOPES, RELAXED UTOPF, LV GRID

Abstract

Distribution System Operators face challenges in managing low-voltage networks due to increasing integration of photovoltaic systems, electric vehicles, and heat pumps. Operating Envelopes, which define the maximum and minimum power limits for end-users, offer a solution for congestion management and flexibility optimization. This paper uses a relaxed unbalanced three-phase Optimal Power Flow method with Second-Order Cone Programming relaxation to compute Operating Envelopes efficiently. By introducing a loss-minimization parameter, λ, the approach balances OE maximization and solution exactness. Case studies on the IEEE EU LV Testfeeder and 49 real LV feeders in Brussels highlight the impact of feeder topology and fairness constraints on OEs. Three feeder types are identified, demonstrating how grid characteristics influence individual and aggregated flexibility. Results confirm that optimal λ selection enhances grid flexibility while ensuring fair and practical OE allocation, supporting DSOs in adapting to evolving network demands.

1 Introduction

Distribution System Operators (DSOs) are facing new challenges to ensure safe use of the low voltage (LV) distribution network with the volume intensification and changes of load profiles. This is due to the integration of new assets such as photovoltaic (PV), electric vehicles (EV) and heat pumps (HP) or the emergence of new activities such as frequency ancillary services or energy sharing newly available on the LV distribution network.

One method used by DSOs to address these challenges consists in computing the maximum and minimum energy yield of LV end users without exceeding congestion constraints. These maximum and minimum power limits, referred to as Operating Envelopes (OEs) [1], can serve as a key tool for congestion management. OEs can be used in several ways, such as through Non-Firm Connection Agreements (NFCA) to limit load profiles during periods of high congestion risk [2], [3]. Alternatively, they can be applied to dynamically pre-qualify LV assets for participation in balancing markets [4].

Recent literature review highlights the need to consider unbalanced three-phases model to compute OEs on the LV distribution network, as strong imbalances can occur, and single-phase models can lead to oversimplification and unexpected congestions [5].

Several methods for calculating an unbalanced three-phase OE currently exist in the literature: e.g. the unbalanced three-phase power flow (UTPF), the unbalanced three-phase optimal power flow (UTOPF) or Machine-Learning techniques [6]. In this paper, a UTOPF method is preferred because the OE should offer more flexibility with the optimization method than with UTPF methods. However, the inherent complexity of the non-convex quadratic OPF equations in UTOPF can result in unacceptably long computation times or non-tractable solutions. To simplify the equations, the model can be approximated, e.g. with a linearization, or relaxed, e.g. with a second-order cone programming (SOCP), a chordal programming (CP) or a semi-definite programming (SDP) [7]. This paper will focus on a UTOPF with SOCP relaxation because this relaxation is the tightest compared to SDP and CP [8]. However, ensuring exactness in OE computation with relaxed UTOPF remains a challenge [9]. To achieve exactness, a loss minimization term is added to the objective function, requiring careful parameterization to maximize the operating envelope while maintaining a valid solution.

The paper begins by briefly presenting the methodology to compute OEs with relaxed UTOPF. The primary contribution lies in analyzing the behavior of OEs influenced by the loss-minimizing parameter and its impact on real-life feeders. Specifically, the study examines how the OEs vary across different network topologies, considering various sizes, impedances, and both star and delta connection models. Real-life feeder scenarios are explored to provide practical insights into the mathematical implications of the relaxation. This is aligned with CIRED's objective of fostering collaboration between academic researchers and DSOs, or other stakeholders.

This work is applied on the IEEE EU LV testfeeder for star connection and using real data from the Brussels LV distribution network, which operates with a delta-connected configuration. In doing so, the paper highlights the influence of network topology on OE calculations.

2 Methodology

This section presents the methodology, as summarized in Figure 1. The process begins with computing OEs for various values of λ using the UTOPF with SOCP relaxation described in **[10]**, and for delta-connected loads in **[11]**.

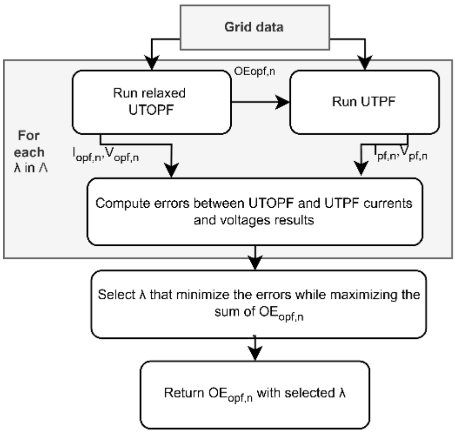

Figure 1: Methodology summary to compute OEs with relaxed UTOPF

The relaxed UTOPF equations are adapted as shown for the power balance equations in (1) and the connection capacity in (2) to consider explicitly $\boldsymbol{OE_c}$ which is the OE per end-user c. The constraint (3) aims to consider the fairness in the model, ensuring that all end-users can access similar relative flexibility.

The objective function defined in (4) aims to optimize the sum of active powers per household to compute the upper OE. To compute the lower OE, the objective function switches from maximization to minimization, and the sign of λ is inverted.

$$\boldsymbol{diag(S_n - z_n L_n) + \sum_{c \in n} OE_c = \sum_{k:n \to k} diag(S_k)} \quad (1)$$

$$\boldsymbol{-s_c^{max} \leq OE_c^{Re} \leq s_c^{max}} \quad (2)$$

$$\boldsymbol{\frac{OE_i^{Re}}{s_i^{max}} = \frac{OE_{i+1}^{Re}}{s_{i+1}^{max}} \quad \forall i \in \mathcal{C}} \quad (3)$$

$$\boldsymbol{\max \sum_{c \in \mathcal{C}} OE_c^{Re} - \lambda \sum_{n \in \mathcal{N}} diag(r_n L_n^{Re})} \quad (4)$$

Here, $\boldsymbol{S_n}$ represents the power branch in branch *n*, $\boldsymbol{z_n}$ is the series impedance matrix and $\boldsymbol{r_n}$ the resistance. $\boldsymbol{L_n}$ denotes the lifted current for branch *n*. The index *k* refers to the possible multiple branches originating from the parent branch *n*. Finally, $\boldsymbol{s_c^{max}}$ represents the maximum connection capacity per end-user.

Other constraints, such as Ohm's Law and the voltage and current limits, are not explicitly represented in the formulation.

For each λ, the UTOPF yields OEs, along with the corresponding current and voltage for each branch and bus. The computed OEs are then used as inputs to an UTPF method to calculate the currents and voltages for each branch and bus. The errors between the current and voltage values obtained from the UTOPF and UTPF methods are subsequently calculated using (5) and (6).

$$\boldsymbol{\frac{1}{n}\sum_{n} |I_{pf_n} - I_{opf_n}|} \quad (5)$$

$$\boldsymbol{\frac{1}{n}\sum_{n} |V_{pf_n} - V_{opf_n}|} \quad (6)$$

The optimal λ, which minimizes losses while maximizing the OEs, is selected to ensure the exactness of the solution. The OEs corresponding to the selected optimal λ is finally chosen.

3 Results

Case studies

This paper discusses two case studies, each with an optimal and a fair scenario. The first case study uses a benchmark distribution grid with a public dataset, enabling the reproduction of results. The second case study analyzes 49 real LV feeders provided by Sibelga in Brussels to derive results based on more realistic data. Finally, the scenario to incorporating fairness is explained and illustrated.

LV distribution grid case studies: Two LV distribution grids are considered. First, the reduced IEEE European LV Testfeeder is chosen as benchmark case study **[12]**: it has 55 single-phase end-users. Each end-user is connected to the grid with a maximum power capacity (in this case: 9.2 kVA). Then, Figure 2 illustrates the second grid studied, which is part of the Sibelga distribution grid in Brussels. It includes 3MV feeders (11kV) connecting 49 LV feeders operating at 230V. The grid serves 2267 end-users across 712 connection points, with some points shared by multiple end-users. Connections are delta-configured and can be single-phase or three-phase, with capacities ranging from 3.7 kVA to 25.1 kVA. End-users are unevenly distributed across feeders and phases, and some have PV systems with known installed and inverter capacities.

Located in an urban area, the grid has an average distance of 13 meters between connection points.

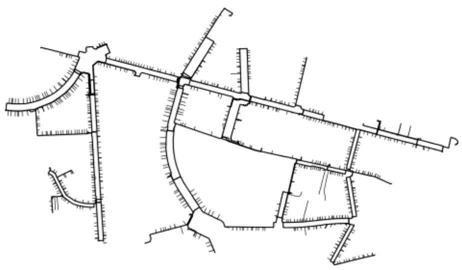

Figure 2: Representation of the 49 Sibelga LV feeders

Fairness scenario: Two fairness scenario are considered, when constraint (3) is not implemented resulting in an optimal but potentially unfair OE, and when the constraint is applied, ensuring all end-users benefit from the same OE capacity.

Results

Selection of λ: The results begins with the selection of λ. Figure 3 illustrates the current values for a single phase across all branches of the IEEE LV Testfeeder, calculated using the UTOPF method and subsequently using the resulting OEs as inputs into the UTPF method. The upper plot represents the results for λ=0, while the lower plot corresponds to λ=5.

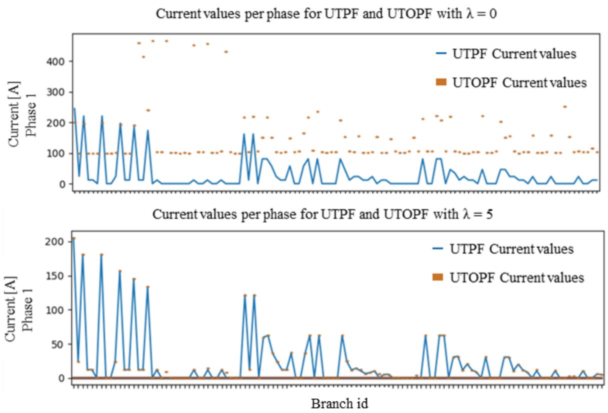

Figure 3: Current values for UTOPF and UTPF for λ=0 and λ=5

When λ=0, loss minimization is not applied, leading to a noticeable error between the UTOPF and UTPF results. This optimal solution allows residual currents to flow in branches where none should exist in a real physical grid. For instance, currents appear on a phase of a branch connected to a household with no load on that phase. In addition, the current values are notably higher in the upper figure compared to the lower one. The upper figure illustrates a solution that lies within the extended feasible set of the lifted variables but does not belong to the original feasible set. This represents a non-exact solution, which is obtained through relaxation, and is not physically realizable in the original problem.

Implementing loss minimization through the λ parameter in the objective function ensures the exactness of the UTOPF solution, aligning UTOPF and UTPF values. Parameterizing λ involves identifying the value of λ that minimizes the error while maximizing the sum of OEs. As illustrated in Figure 4 , when λ=0, the sum of OEs is at its highest, but this also corresponds to the largest error. As λ increases, the error decreases, but the sum of OEs also declines due to the increasing weight of loss minimization in the objective function, which reduces the overall OEs.

The optimal λ is the value that minimizes the error (e.g., λ={2,5,15,20}) while achieving the highest possible sum of OEs to unlock greater flexibility. Consequently, λ=2 or λ=5 are the most suitable choices.

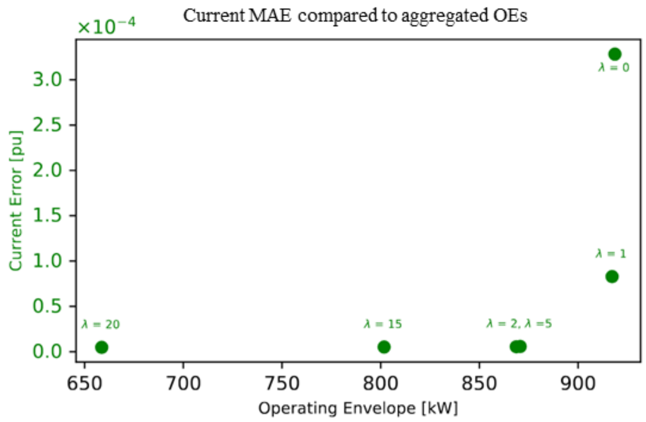

Figure 4: Current MAE compared to aggregated OE

OE results: After selecting the λ values, the OE results can be computed. These OE values are summarized in Table 1 for both the IEEE EU LV Testfeeder and the 49 Sibelga feeders.

Table 1: OE results

Grid	Metrics	Optimal UTOPF	Fair UTOPF
IEEE EU LV feeder	OE	110.1 %	100%
	Current MAE [p.u.]	0.001	0.001
	Voltage MAE [p.u.]	0.004	0.013
Sibelga LV feeders	OE	119.2%	100%
	Avg. Current MAE [p.u.]	0	0
	Avg. voltage MAE [p.u.]	0.006	0.007
	Max. voltage MAE [p.u.]	0.013	0.018

This paper aims to provide a deeper understanding of how OEs behave in relation to specific LV feeder topologies. Three distinct types of LV feeders are identified and illustrated in this study. In the following figures, each pair of bars represents the OE limit for an end-user, where "end-user" refers to the aggregated group of end-users behind the same connection point. The dark green bar represents the optimal OE per connection point, the light green bar represents the fair OE, and the light yellow bar represents the maximum connection capacity. Both the optimal and fair OEs cannot exceed the maximum connection capacity (see (2)).

Feeder type 1 – Oversized feeders. These feeders are characterized by their maximum power not being constrained by grid cables capacity but rather by the connection capacities, as defined in (2). This behavior is illustrated in Figure 5, where both the Optimal and Fair OEs consistently reach the maximum connection capacity. Out of the 49 LV feeders provided by Sibelga, 15 fall into this category, serving between 1 and 24 end-users over lengths ranging from 24 meters to 222 meters

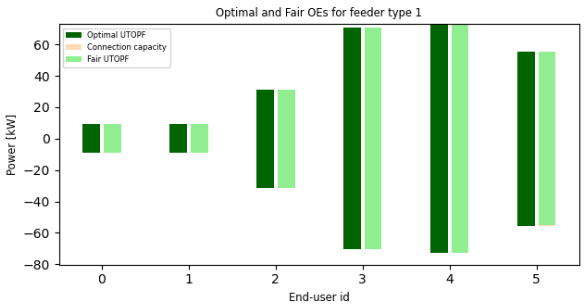

Figure 5: OE on LV feeder of type 1

Feeder type 2 – Feeders where fairness does not reduce aggregated OEs. In this case, the fairness principle does not reduce the total flexibility available on the feeder. While individual OEs for specific end-users may vary, the aggregated OE at the feeder level remains similar. This is demonstrated in Figure 6. For example, for end-user 0, located near the head of the feeder, the Optimal OE allows access to the maximum power, while the Fair OE reduces it. Conversely, for end-user 13, situated at the end of the feeder, the Optimal OE is more restricted compared to the Fair OE. Despite these individual variations, the total sum of OEs across all end-users on the feeder remains consistent between the Optimal and Fair methods.

Feeder type 3 – Other feeders. This category includes feeders that do not fit the characteristics of Types 1 or 2. Their behavior is illustrated in Figure 7.

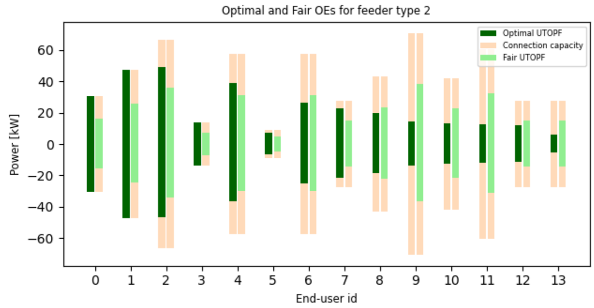

Figure 6: OE on LV feeder of type 2

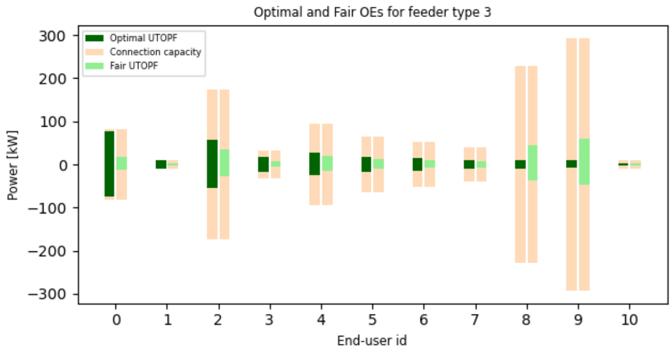

Figure 7: OE on LV feeder of type 3

Topology analysis: Several topological characteristics of the real Sibelga LV feeders are analyzed and compared with feeder types and λ values. The analyzed characteristics include the nominal capacity of the feeder [kVA], the total connection capacity [kVA] (TCC), the total feeder length [m] and the maximum branch length [m] (MBL). To evaluate the statistical significance of differences in these characteristics across feeder types, non-parametric tests are conducted.

The Kruskal-Wallis test reveals that both the MBL ($p=0.012$) and TCC ($p=0.006$) exhibit significant differences across feeder types. Pairwise comparisons using the Mann-Whitney U test show that for the MBL, a significant difference exists between Feeder Type 1 and Feeder Type 2 ($p=0.005$). For TCC, significant differences are observed between Feeder Type 1 and Feeder Type 2 ($p=0.025$) as well as between Feeder Type 1 and Feeder Type 3 ($p=0.002$).

Figure 8 illustrates statistical distribution per feeder type. For MBL, Feeder type 1 has the highest median, with greater variability compared to Feeder types 2 and 3. In contrast, TCC is higher in Feeder types 2 and 3 compared to type 1, with type 3 showing the most consistent distribution. These findings emphasize that both features—Maximum Branch Length and

Total Connection Capacity—are key in distinguishing feeder types and understanding their operational characteristics.

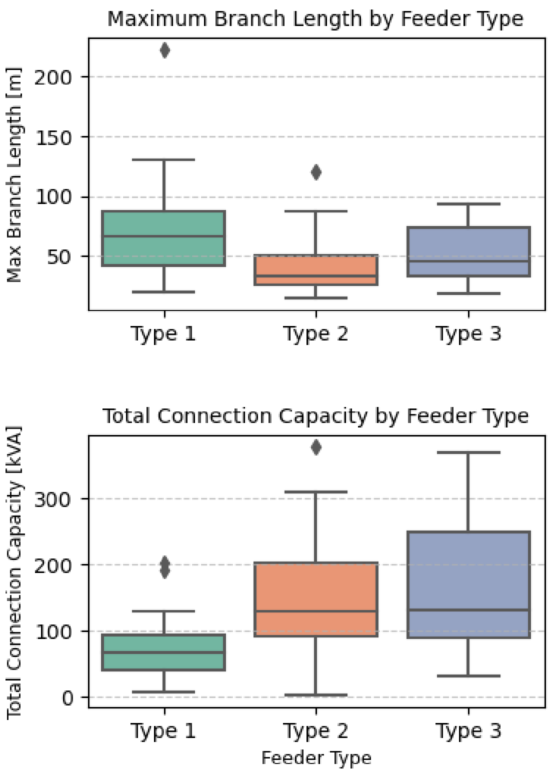

Figure 8: Boxplots for significant topological characteristics

4 Conclusions

This paper explores practical considerations for OEs computation in LV distribution networks while maximizing flexibility. Using a relaxed UTOPF approach with SOCP and incorporating a loss-minimization term, the study ensures both accurate and optimal OE computation. Case studies demonstrate how λ parameterization balances error reduction and OE maximization, providing a robust framework for efficiently managing grid constraints and enhancing network flexibility.

The analysis of 49 real LV feeders and the IEEE EU LV Testfeeder identifies three distinct feeder types, offering practical insights into the interaction between network topology and OEs. Oversized feeders can achieve their maximum OE without risking congestion on the grid, while Type 2 feeders highlight the trade-offs between fair and optimal flexibility without reducing total aggregated OEs. A statistical examination of topological characteristics underscores the relevance of Maximum Branch Length and Total Connection Capacity in distinguishing feeder types, reinforcing their influence on OE performance and network design.

This work provides DSOs with a robust methodology for tailoring OE calculations to diverse network scenarios, equipping them to manage increasing renewable integration, changing load profiles, and the growing demand for grid services. Future work should explore the dynamic adjustment of OEs and incorporate stochastic modeling to account for uncertainty in renewable generation and load behavior.

5 Acknowledgements

This study is conducted under the framework of the federal Belgian project named ALEXANDER, funded by the Energy Transition Fund of the Federal Public Service (FPS) Economy of Belgium.

6 References

[1] DEIP (Dynamic Operating Envelopes Working Group), "Outcomes report," 2022. [Online]. Available: https://arena.gov.au/assets/2022/03/dynamic-operating-envelope-working-group-outcomes-report.pdf. [Accessed 2024].

[2] M. Z. Liu, L. F. Ochoa, P. K. Wong and J. Theunissen, "Using OPF-Based Operating Envelopes to Facilitate Residential DER Services," *IEEE Transactions on Smart Grid*, vol. 13, no. 6, pp. 4494-4504, 2022.

[3] Bundesnetzagentur, "Bundesnetzagentur launches second consultation on integrating controllable consumer devices into the electricity grid," 2023. [Online]. Available: https://www.bundesnetzagentur.de/SharedDocs/Pressemitteilungen/EN/2023/20230616_Sperrfrist.html. [Accessed 2024].

[4] A. Kaushal, W. Ananduta, L. Marques, T. Cuypers and A. Sanjab, "Operating envelopes for the grid-constrained use of distributed flexibility in balancing markets," in *ISGT*, 2024.

[5] B. Liu and J. H. Braslavsky, "Sensitivity and Robustness Issues of Operating Envelopes in Unbalanced Distribution Networks," *IEEE Access*, vol. 10, pp. 92789-92798, 2022.

[6] L. Bin and J. H. Braslavsky, "Robust Dynamic Operating Envelopes for {DER} Integration in Unbalanced Distribution Networks," *IEEE Transactions on Power Systems*, vol. 39, no. 2, pp. 3921-3936, 2024.

[7] K. D. Molzahn and A. I. Hiskens, A Survey of Relaxations and Approximations of the Power Flow Equations, Now, 2019.

[8] L. Gan and H. S. Low, "Convex relaxations and linear approximation for optimal power flow in multiphase radial networks," in *2014 Power Systems Computation Conference*, 2014.

[9] S. H. Low, "Convex Relaxation of Optimal Power Flow—Part II: Exactness," *IEEE Transactions on Control of Network Systems*, vol. 1, no. 2, pp. 177--189, 2014.

[10] L. Gan, U. Topcu, N. Li and S. H. Low, "Exact convex relaxation of OPF for radial networks using branch flow model," in *2012 IEEE Third International Conference on Smart Grid Communications (SmartGridComm)*, 2012.

[11] S. H. Low, C. Zhao and E. Dall'Anese, "Optimal Power Flow in Multiphase Radial Networks with Delta Connections," in *IREP 2017 Bulk Power Systems Dynamics and Control Symposium*, 2017.

[12] M. A. Khan and P. B. Hayes, "A Reduced Electrically-Equivalent Model of the IEEE European Low Voltage Test Feeder," in *2022 IEEE Power and Energy Society General Meeting (PESGM)*, 2022.